Equivalent Sources: Rapid Calculation in the Frequency Domain and Application to Leveling Correction

Dean Hillan
CSIRO Earth Science and Resource Engineering
Sydney, Australia
dean.hillan@csiro.au

Phil Schmidt
CSIRO Earth Science and Resource Engineering
Sydney, Australia
phil@magneticearth.com.au

SUMMARY

The equivalent source is usually calculated by an iterative method, designed to converge on the observed potential field, magnetic or gravitational. Each iteration involves two Fourier transforms, one forward and one inverse. As the number of grid point increases the time penalty may become prohibitive. However, the number of transforms can be dramatically reduced by the *a priori* transformation of the observed potential field to the frequency domain. We describe this method which reduces the number of Fourier transforms from *n* to two, and demonstrate its use on a simple magnetic anomaly. An extension of this equivalent source technique is also given for the case of a draped magnetic survey that requires leveling correction. The observed data is separated into layers according to the height changes, and the equivalent source is iteratively calculated via comparisons of the upward continued data. Whilst this process is computationally intensive, it is designed to scale with the complexity, and hence the discretisation, of the topographical changes. This gives the method a speed advantage compared with similar Taylor series approaches. A synthetic example containing multiple dipole sources is used to test the method, and to illustrate the advantages and differences of draped surveys and the need to reduce the data to a common datum.

Key words: Equivalent layer, magnetic survey, Fourier techniques, draped survey

INTRODUCTION

The calculation of equivalent sources provides a very flexible tool for recalculating many varieties of fields and gradients, such as the analytic signal, first vertical derivative and the magnetic gradient tensor. Since equivalent sources techniques were first described (Dampney, 1969) they have found application in processing and filtering of potential field data (Emilia, 1973), and to aid in geological mapping by constraining the source of magnetisation (Pilkington, 1998). We describe a rapid equivalent source technique in the next section for the magnetic case, where the data is observed on a flat plane.

Airborne potential field surveys may be designed such that the distance between the sensor and the ground is held approximately constant as opposed to flying at a fixed altitude. These are known as 'draped' surveys. A draped survey may have better resolution for separating sources as the distance from the source is minimised and the magnetic field falls off rapidly with height. However, such data may contain artefacts and distortions of anomaly patterns that should be corrected by applying leveling (Cowan and Cooper, 2003; Pilkington and Roest, 1992; Xia et al. 1993) and topological corrections (Pilkington, 1998). We also describe how equivalent sources may be used to rapidly make these corrections, again applied to the magnetic case.

EQUIVALENT SOURCE METHOD

We use an iterative method similar to that of Xia et al. (1993) to calculate equivalent sources for total magnetic intensity (TMI) data observed on a flat plane. The speed of the calculation can be greatly improved by transforming to the Fourier domain, iteratively calculating the equivalent source $J(\mathbf{K})$ and then transforming back to Euclidean space. All convergence is carried out in the frequency domain and this requires only two transforms in total, rather than one for each iteration as the source layer is updated as per Xia et al. (1993). The process is described below.

The Fourier transform $O(\mathbf{K})$ of the observed data $O(x, y)$ is calculated, where the observed data is a TMI grid recording the intensity variation projected onto the Earth's field, which has a directional component vector $\boldsymbol{f}$. In general we do not know the magnetisation direction $\boldsymbol{m}$ and it is assumed that $\boldsymbol{m}=\boldsymbol{f}$. The quantities Θ_m and Θ_f are then formed from the product of the vectors $\boldsymbol{m} = (m_x, m_y, m_z)$ and $\boldsymbol{f} = (f_x, f_y, f_z)$, and the components of the wave vector $\boldsymbol{k}$ in the Fourier domain such that

$$\Theta_m = m_z + i\frac{m_x k_x + m_y k_y}{|k|} \tag{1}$$

$$\Theta_f = f_z + i\frac{f_x k_x + f_y k_y}{|k|} \tag{2}$$

(Blakely, 1996). The iterative calculation proceeds using

$$T^n(\mathbf{K}) = 2\pi\Theta_m\Theta_f J^n(\mathbf{K}) \tag{3}$$

to forward compute the TMI response at the *n*-th iteration, and

$$J^{n+1}(\mathbf{K}) = J^n(\mathbf{K}) + C(O(\mathbf{K}) - T^n(\mathbf{K})) \tag{4}$$

to update the equivalent source layer with the difference between the current response and the observed response, where C is a constant chosen for convergence (Xia et al. 1993). At the zero-th iteration we begin with $J(\mathbf{K})^0 = 0$ and

the iterations continue until the RMS change to the equivalent layer at the n-th step converges to below some threshold. After convergence, the inverse Fourier transform of $J(\mathbf{K})$ may be calculated yielding the equivalent layer $J(x, y)$ or instead be used to generate transforms or derivatives of the field.

Example

Figure 1 (top left) shows a TMI image of an induced anomaly in a declination 0° and inclination -60° field. This grid is 41x41 points, and represents the observed data $O(x, y)$ for which we calculate the equivalent layer using the above method. The remaining panels of Figure 1 show the forward computed TMI grid from (3) at iteration number 1, 10, and 20. Comparison of these grids with the original observed data shows convergence towards the observed TMI.

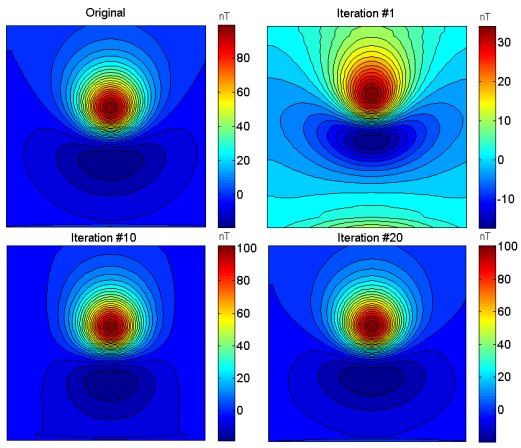

Figure 1. A series of plots showing the equivalent layer calculation converging to the original observed TMI grid (top left). Grids are plotted for iteration number 1 (top right), 10 (bottom left), and 20 (bottom right).

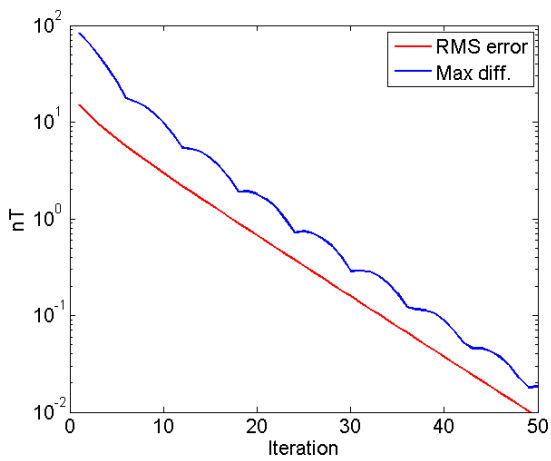

Figure 2. A plot of the misfit statistics as a function of iteration number for the calculation of the equivalent source for the example in Figure 1.

Figure 2 shows the reduction in the root mean squared (RMS) and maximum differences between the forward computed TMI from the equivalent layer and the original observed data as a function of iteration number. Sufficient accuracy is obtained after 50 iterations, where we have used C=0.07 in (4). Different values of C produce different convergence rates.

Plots of the final TMI image and the associated equivalent layer are shown in Figure 3.

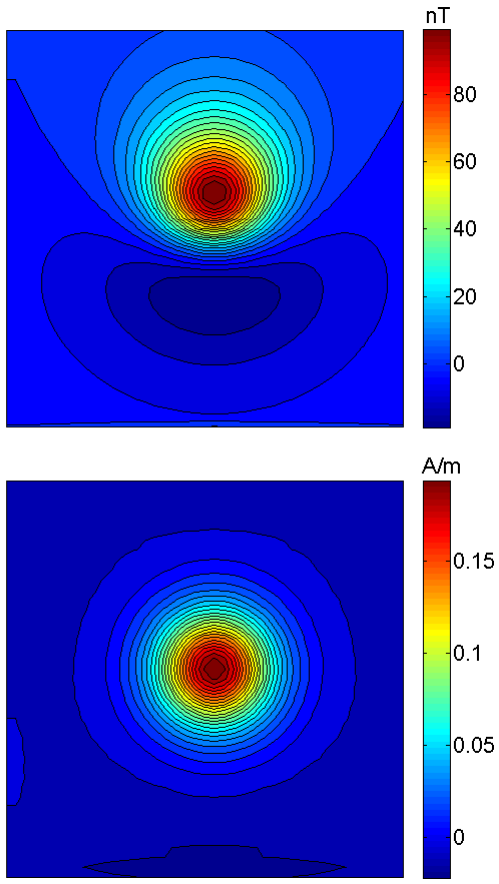

Figure 3. Plots of the final TMI image at 50 iterations (top panel) computed from the final equivalent layer (bottom panel) for the example in Figure 1.

LEVELING CORRECTION

Draped surveys have the advantage of superior source separation, but corrections are required to address any distortion that is introduced. Ideally the data would be reduced to a plane surface as low to the ground as possible. Figure 4 (top left) plots observed TMI on an ideal plane surface at 60m height (-60m depth) over five dipole sources, and shows good separation of each of the sources.

In the case of a topological high in the survey area, such as that modelled in Figure 5, obtaining level data at 60m height is precluded by the 100m rise. A fixed altitude survey might instead be flown at a higher altitude of 160m which gives the observed TMI in Figure 4 (bottom right). At this altitude there is a weaker signal and poor separation of the sources. Figure 4 (top right) shows an ideal draped survey, which maintains a fixed distance of 60m to the grounds surface at all times, and shows superior resolution to the high altitude survey.

Whilst a draped survey is intended to maintain a constant distance between the sensor and the ground, the actual flight path may vary more smoothly than the topology and be subject to small altitude fluctuations. We model these effects for a 'realistic' draped survey whose path follows the blue surface in Figure 5 and yields the observed TMI plotted in Figure 4 (bottom left). The TMI for the realistic drape is

somewhat inferior compared with the ideal drape, but still superior to the high altitude TMI. We apply leveling corrections to the realistic draped TMI below, using the modelled flight path in Figure 5.

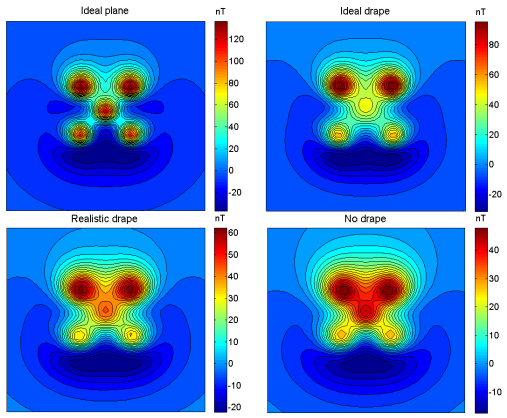

Figure 4. A series of panels showing observed TMI data over five dipole sources with different heights and drapes. (Top left) An ideal plane surface at 60m height. (Top right) An ideal drape at 60m above the grounds surface. (Bottom left) A realistic drape that varies more smoothly than the grounds surface, as in Figure 5. (Bottom right) A plane surface at 160m height.

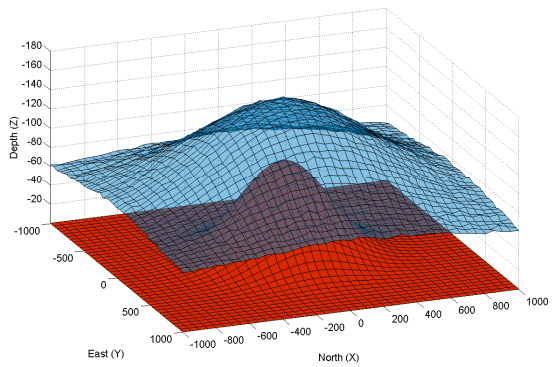

Figure 5. The flight path of a modelled draped survey (blue surface) over the ground (brown surface) containing topological relief.

APPLICATION OF EQUIVALENT SOURCES

The equation for calculation of a topologically varying magnetisation to a flat observation plane is given by Parker (1973) and involves a Taylor expansion of the height function. Inverse formulations of this equation can be used to find the equivalent source layer (Pilkington 1998, Xia et al. 1993). Whilst the Fourier computations are efficient, the number of terms in the Taylor series required for convergence may increase with increasing grid points, and each requires an inverse Fourier transform. As the number of points increases, the computation time may become prohibitively large.

The method we propose below relies on breaking the flight path topology of the observation up into discrete layers, and then forward computing a number of upward continuations from the same source. A correction is then made to the equivalent source based on the difference between the forward computed data and the observed data, and the process continues in an iterative fashion. In this method, the computation time is reliant on the discretisation of the flight path and hence the topological complexity, where in the limit of a flat flight path we arrive at an analogous method to that described in the previous section for a flat observation plane.

We wish to calculate the equivalent source $J(x, y)$ at a depth just below the minimum altitude of the draped survey Z_0. The observed TMI grid is distributed to multiple layers according their height h above Z_0. Figure 6 visualises these layers for the realistic drape example of the previous section with the equivalent layer placed at Z_0=-60m depth, and the layer thickness set to 20m.

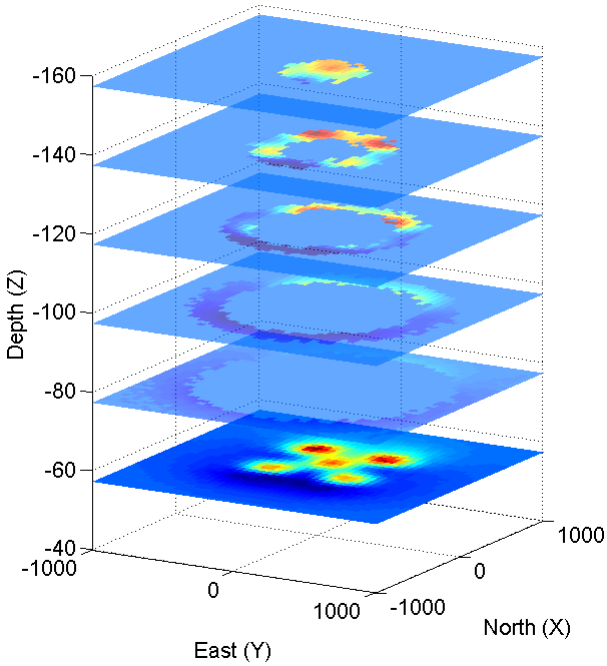

Figure 6. A visualisation of the observed TMI data layered into planes of varying height for the modelled flight path in Figure 5. The plane at -60m depth is the equivalent source layer.

The forward computed TMI at n-th iteration for the i-th layer is given by

$$T_i^n(\mathbf{K}) = 2\pi\Theta_m\Theta_f J(\mathbf{K})e^{-h_i|\mathbf{k}|} \tag{5}$$

and the equivalent layer is updated via

$$J^{n+1}(\mathbf{K}) = J^n(\mathbf{K}) + \Sigma_i C(O_i(\mathbf{K}) - T_i^n(\mathbf{K})) \tag{6}$$

where again C is a constant chosen for convergence. Note that the points on each layer that contain observation data only form a subset of each layer, and the remaining points are set to zero. The final TMI data is forward computed from the equivalent source at the median height of the survey as in Xia et al. (1993).

For the example of the modelled realistic drape, the median flight height is -87m depth and the final calculated TMI image, using a observation layer thickness of 10m (12 layers), is plotted in the top panel of Figure 7 with the correct ideal plane grid at -87m depth plotted in the bottom panel (i.e. akin to the top left panel of Figure 4 upward continued by 27m). The iterative process was truncated when the RMS change in

the equivalent layer fell below 0.001nT. Further calculation leads to decreasing errors but enhancement of the shorter wavelength features, as in downward continuation. In practice some sort of smoothing or wavelength filtering should be employed.

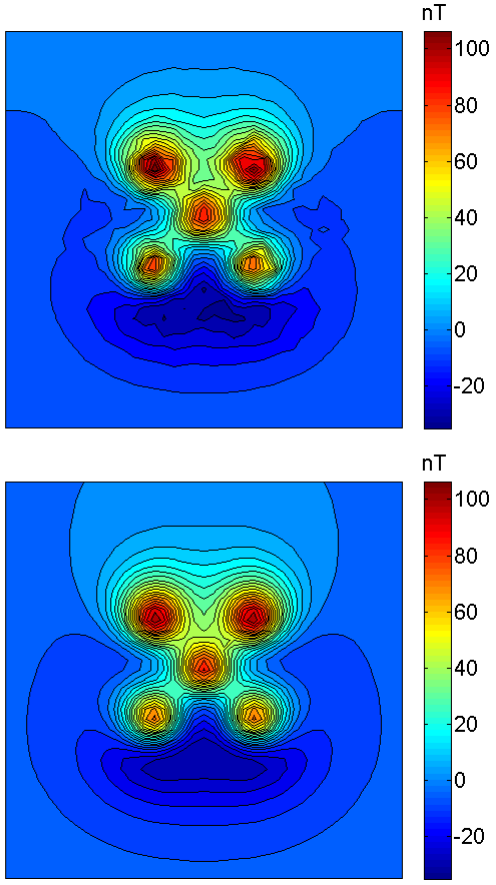

Figure 7. Plots showing the calculated TMI in Figure 4 (bottom left) corrected for leveling and the ideal plane TMI for the five dipole source example, both at -87m depth (87m height).

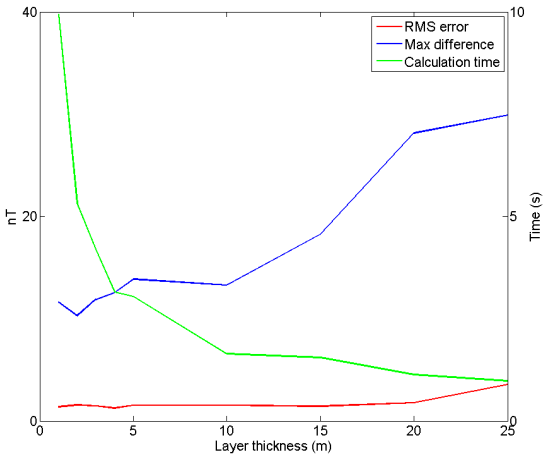

Figure 8. A plot of the RMS misfit between the level adjusted draped TMI and the correct TMI as a function of layer discretisation thickness.

The RMS and maximum differences between the two grids in Figure 7 is 1.54nT and 13.29nT, respectively. This error tends to decrease with increasing height discretisations, whilst the calculation time increases. This effect is summarised in Figure 8. Since the standard deviation in the flight path height is 26m, this plot suggests that a discretisation equal to around half of this variability in flight path topology provides a good trade off between accuracy and the computational effort required.

CONCLUSIONS

A method for rapidly calculating equivalent sources in the Fourier domain is presented and applied to a simple synthetic example. This equivalent source may then be used to calculate a range of field transforms or derivatives. An extension to the basic equivalent source method is given where leveling corrections may be applied to a draped survey by discretising the observed data into layers by height. This method is successfully applied to a modelled draped survey over five dipole sources and the data is reduced to a common datum. The method is fast and converges to a grid which closely resembles the correct result. Future extensions should also include a correction for topology in order to map magnetisations on a surface.

ACKNOWLEDGMENTS

This research is supported by CSIRO capability development funding.

REFERENCES

Blakely, R. J., 1996, Potential Theory in Gravity and Magnetic Applications: Cambridge University Press.

Cowan, D., and Cooper, G., 2003, Drape related problems in Aeromagnetic Surveys: The need for tight-drape surveys, ASEG abstracts 2003 (1), 1-4.

Damney, C., 1969, The equivalent source technique: Geophysics 34, 39-53

Emilia, D., 1973, Equivalent sources used as an analytic base for processing total magnetic field profiles: Geophysics 38, 339-48.

Parker, R., 1973, The rapid calculation of potential anomalies: Geophysical Journal of the Royal Astronomical Society, 31 (4), 447-455.

Pilkington, M., 1998, Magnetisation mapping in rugged terain: Exploration Geophysics 29, 560-564.

Pilkington, M., and Roest, W.,1992, Draping aeromagnetic data in areas of rugged topography: Jour. Appl. Geophys. 29, 135-142

Woodward, D., 1993, Inversion of aeromagnetic data using digital terrain models: Geophysics 58, 645-652.

Xia, J., Sprowl, D.R., and Adkins-Heljeson, D., 1993,Correction of topographic distortions in potential-field data: A fast and accurate approach: Geophyics 58 (4), 515-523